

Fundamental Three-Dimensional Configuration of Wire-Wound Muscle-Tendon Complex Drive

Yoshimoto Ribayashi¹, Yuta Sahara¹, Shogo Sawaguchi¹, Kazuhiro Miyama¹, Akihiro Miki¹, Kento Kawaharazuka¹, Kei Okada¹, and Masayuki Inaba¹

Abstract—For robots to become more versatile and expand their areas of application, their bodies need to be suitable for contact with the environment. When the human body comes into contact with the environment, it is possible for it to continue to move even if the positional relationship between muscles or the shape of the muscles changes. We have already focused on the effect of geometric deformation of muscles and proposed a drive system called wire-wound Muscle-Tendon Complex (ww-MTC), an extension of the wire drive system. Our previous study using a robot with a two-dimensional configuration demonstrated several advantages: reduced wire loosening, interference, and wear; improved robustness during environmental contact; and a muscular appearance. However, this design had some problems, such as excessive muscle expansion that hindered inter-muscle movement, and confinement to planar motion. In this study, we develop the ww-MTC into a three-dimensional shape. We present a fundamental construction method for a muscle exterior that expands gently and can be contacted over its entire surface. We also apply the three-dimensional ww-MTC to a 2-axis 3-muscle robot, and confirm that the robot can continue to move while adapting to its environment.

I. INTRODUCTION

Humanoid robots have been actively developed by companies in recent years [2]–[5], achieving dexterous manipulation and stable locomotion. Most of the robots presented have rigid bodies, and they deal with environmental contact only at the end-effectors, such as hands and feet. As for contact with other parts of the body, although there are some examples of studies on multi-point contact [6]–[8] and disturbances applied during push recovery motions [9]–[11], the topics covered are limited. For example, complex movements involving whole-body surface contact, such as holding with arms and torso, or pushing aside obstacles with the body while both hands are occupied, are challenging to achieve. If the robot tries to force its body to move when it is in contact with the environment, its rigid body may damage the surrounding environment. In order for robots to play a more active role in society, it is necessary for robots to handle a broader range of environmental contacts and to have a body suitable for such contacts.

There are soft humanoids that fit into the environment, such as those using a wire drive [12]–[14] and those using pneumatic artificial muscles [15], [16]. Although each drive method has its own advantages and disadvantages, we focus

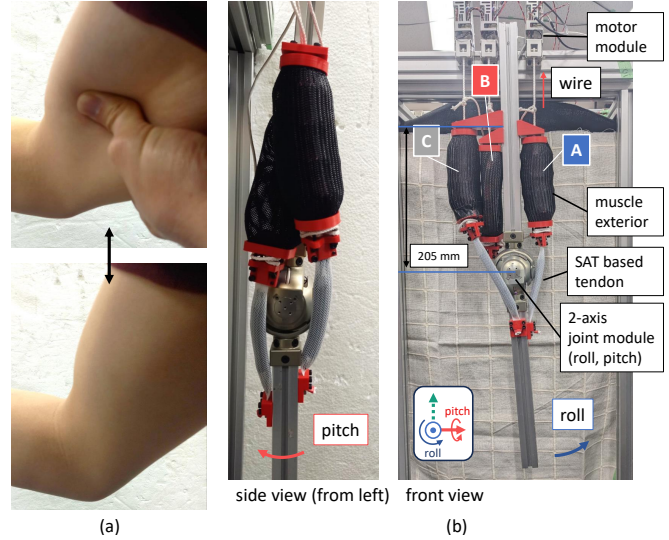


Fig. 1. (a) Muscle-tendon complexes adjust their shape and internal spatial relationships when encountering contact, enabling continued movement while adapting to the environment. They return to their original position after contact with the environment ends. (b) 2-axis 3-muscle robot with three-dimensional configuration.

on the wire drive in this research. The major advantage of the wire drive is that it exerts a large force and its high controllability due to the winding by the motor. However, handling environmental contact with the entire body is challenging because of unexpected interference and loosening of the wires in a body configuration with exposed wires. Humanoids need bodies that can adapt to the environment like humans do. They must also be able to operate while making good use of the environment by contacting all body surfaces and continuing to operate safely in the face of environmental disturbances.

The human body’s remarkable adaptability to environmental contact is primarily due to its muscle-tendon complexes. These complexes not only provide flexibility but also enable dynamic adaptation to external forces. When encountering environmental contact, muscle-tendon complexes can adjust their shape and spatial relationships between muscles and tendons. This adaptability allows for continued movement while conforming to new environmental conditions. Moreover, they quickly return to their original positions and shapes when contact ceases (Fig. 1(a)). In this study, we focus on these adaptive characteristics to develop a body-driving system that is highly adaptable to environmental contact.

We have already proposed a drive system called the wire-wound Muscle-Tendon Complex (ww-MTC), which incorpo-

¹ The authors are with the Department of Mechano-Informatics, Graduate School of Information Science and Technology, The University of Tokyo, 7-3-1 Hongo, Bunkyo-ku, Tokyo, 113-8656, Japan. [ribayashi, sahara, sawaguchi, miyama, miki, kawaharazuka, k-okada, inaba]@jsk.t.u-tokyo.ac.jp

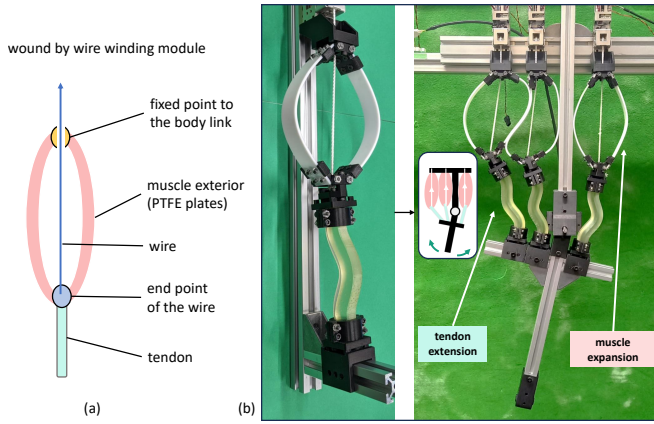


Fig. 2. (a) Conceptual diagram of wire-wound Muscle-Tendon Complex drive [1]. (b) 1-axis 3-muscle robot with two-dimensional configuration [1].

rates muscle-tendon deformation into the wire drive [1](Fig. 2). The concept of incorporating geometrical shape changes of muscles in a two-dimensional configuration is realized, and advantages such as prevention of wire loosening, securing of moment arms, internal protection against environmental contact, and muscular appearance are confirmed. This method is similar to pneumatic artificial muscles such as the McKibben type [17], [18] in that it expands with contraction. However, since the tension is provided by an internal wire, the shape can be changed in various ways according to the design of the muscle exterior. This study concludes that the incorporation of muscle expansion is promising for body configurations suitable for environmental contact. On the other hand, this configuration has the problem of too large expansions of the muscle parts inhibiting each other's movement. In addition, developing a three-dimensional muscle exterior that has no gaps on its surface and can expand and deform has been a major challenge.

In order to use muscle-tendon complex drives in three-dimensional movements and body configurations, we develop muscle exterior and tendon elements with more compact shapes and entirely covered surfaces. In particular, for muscles that expand and deform, we propose a structure consisting of a frame made of arch-shaped material that defines the deformation and a braided sleeve that covers the surface. In addition, the proposed structure's effectiveness is verified by performing motion experiments with environmental contact on a 2-axis, 3-muscle robot using a three-dimensional ww-MTC.

The main contributions of this study are as follows:

- This study shed light on the inherent adaptability of deformable biological muscles during environmental contact and aimed to achieve it in robotic systems.
- We proposed a structure that deforms three-dimensionally under wire tension, and confirmed the relationship between contraction distance and expansion through theoretical calculations.
- We have verified that the robot using 3D ww-MTC maintains its operation even if the position and shape of the muscles change during environmental contact.

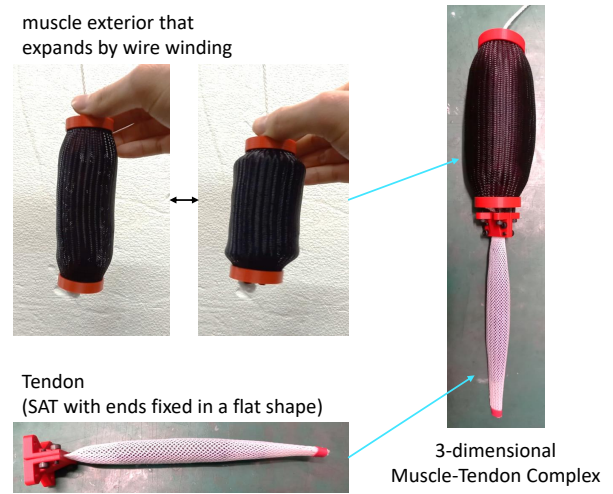


Fig. 3. Three-dimensional ww-MTC consists of the muscle exterior and the tendon based on Stiffness Adjustable Tendon (SAT) [20].

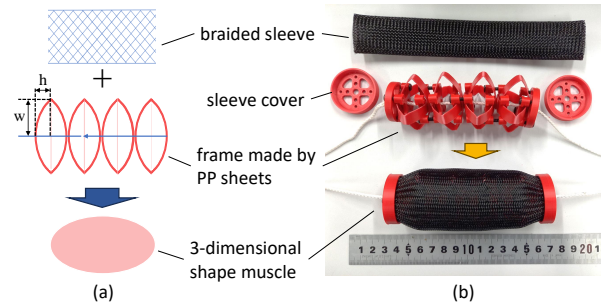


Fig. 4. (a) Conceptual diagram of three-dimensional muscle. Muscle exterior is made by frame determining shape change and braided sleeve covering the surface. (b) Assembly of the muscle exterior.

II. 3D CONFIGURATION OF A WIRE-WOUND MUSCLE-TENDON COMPLEX DRIVE

The three-dimensional muscle exterior requires the following.

- The entire body surface is covered and contactable, i.e., usable in three-dimensional movements.
- The muscle expansion is gentle and does not interfere with the movement of other muscles.

Tendons made of rubber are large compared to their strength, and have problems with deterioration and rupture [1]. Therefore, the following tendon requirements are set.

- The tendon is thin enough.
- The tendon is strong enough.
- The friction on the tendon's surface is small and does not interfere with contact at joints.

The level of detail in these tendon requirements depends on factors such as the size of the joint modules [14] and the performance of the motor modules [19] used in this study. Based on the above requirements, we propose a ww-MTC that can be used in a three-dimensional configuration (Fig. 3).

For the winding of the wire, we use a wire winding module developed in our laboratory [19]. This module can wind the

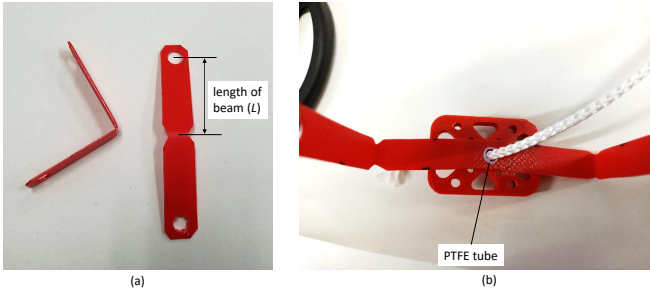


Fig. 5. The PP sheet is processed as shown in (a). The distance from the hole through which the wire passes to the seam corresponds to the length of the beam and is an important parameter that defines the deformation of the muscle exterior. (b) PTFE tube is inserted to prevent wires from getting stuck.

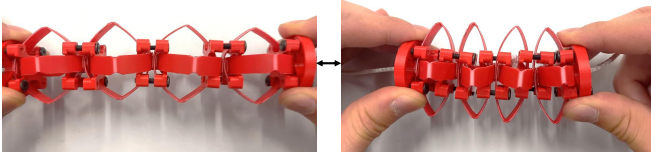


Fig. 6. The image shows the deformation of the frame. The width becomes a little larger as the length becomes shorter.

wire by rotating the motor, and only the current is controlled in this study. The tension value is measured by the on-board load cell.

A. Muscle Exterior

1) *Muscle Exterior Construction Method:* In this study, a three-dimensional muscle exterior was developed by covering a frame made of polypropylene (PP) sheet, which deforms according to wire winding and determines the overall shape, with a braided sleeve (Fig. 4).

First, PP sheets are processed as shown in Fig. 5(a). The PP sheets are easy to process because a laser machine can cut them. At the part where the wires are threaded through the PP sheet, a slippery polytetrafluoroethylene (PTFE) tube is inserted to prevent the wires from rubbing against the PP sheet and getting entangled (Fig. 5(b)). By arranging multiple arch-shaped materials as a frame, the deformation per unit shrinkage distance is reduced, and a gentle expansion is achieved. Fig. 6 illustrates the frame's deformation as the muscle contracts, showing how the width increases slightly as the length decreases. The arches are covered with braided sleeves and fixed at both ends so they can be contacted on all surfaces.

2) *Theoretical Calculations of Deformation:* The deformation of the PP sheet, which constitutes the frame part of the muscle exterior developed in this research, can be modeled as a large deformation of a cantilever beam subjected to a concentrated vertical load at the free end. This can be calculated by material mechanics [21]. In the following, we summarize the beam's deformation for theoretical verification of the deformation of the developed exterior.

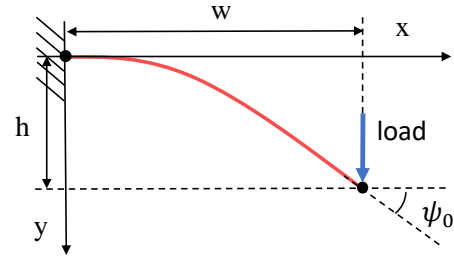


Fig. 7. Flexible bar (based on the figure 2.2 of [21])

The elliptic integrals of the first and second kind, and the complete elliptic integrals of the first and second kind can be written as follows:

$$F(\phi, p) = \int_0^\phi \frac{d\theta}{\sqrt{1-p^2 \sin^2 \theta}} \quad (1)$$

$$E(\phi, p) = \int_0^\phi \sqrt{1-p^2 \sin^2 \theta} d\theta \quad (2)$$

$$K(p) = F\left(\frac{\pi}{2}, p\right) = \int_0^{\pi/2} \frac{d\theta}{\sqrt{1-p^2 \sin^2 \theta}} \quad (3)$$

$$E(p) = E\left(\frac{\pi}{2}, p\right) = \int_0^{\pi/2} \sqrt{1-p^2 \sin^2 \theta} d\theta \quad (4)$$

In this case, the width w and height h of the beam (Fig. 7) can be calculated using the beam length L and the shape parameter p (where $1/\sqrt{2} \leq p < 1$) as follows [21]:

$$w = \frac{1}{k} \sqrt{2(2p^2 - 1)} \quad (5)$$

$$h = \frac{1}{k} \{K(p) - F(\phi_1, p) - 2E(p) + 2E(\phi_1, p)\} \quad (6)$$

Where k and ϕ_1 are defined as:

$$k = \frac{K(p) - F(\phi_1, p)}{L} \quad (7)$$

$$\phi_1 = \sin^{-1} \left(\frac{1}{\sqrt{2p}} \right) \quad (8)$$

Additionally, the shape parameter p is related to the angle ψ_0 between the beam tip and the horizontal direction as follows:

$$\sin \psi_0 = 2p^2 - 1 \quad (9)$$

3) *Deformation of Muscle Exteriors:* In this study, we have developed two types of exterior: one achieves radial expansion in the plane perpendicular to the contraction, and the other exhibits unidirectional expansion perpendicular to the contraction (referred to as planar muscle in this study). We verify the measured results of actual deformations with theoretical calculations for these two types of muscles. The length shown in Fig. 5(a) corresponds to the length L of the beam. The theoretical calculations of w and h correspond to the width and length shown in Fig. 4(a).

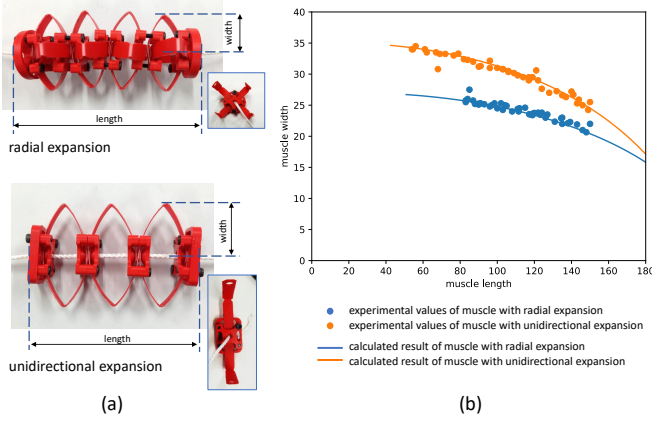


Fig. 8. (a) Two types of frames made of PP sheets. (b) Lines show calculated values, plots show experimental values. Calculated result is representing the experimental result well.

The difference in shape is realized by changing the direction of the arch structure in the frame, four directions in the former and two directions in the latter (Fig. 8(a)). Let n be the number of arches in the length direction and h_0 be the offset due to sheet thickness and components, then the width and length of the muscle exterior are multiplied using Eq. (5) and Eq. (6) as follows:

$$(width) = w(L, p) \quad (10)$$

$$(length) = n \times h(L, p) + h_0 \quad (11)$$

For the muscles with radial expansion, $n=8$, $L=27$ mm, $h_0=22$ mm. For the planar muscles, $n=6$, $L=35$ mm, $h_0=14.5$ mm. These values were determined experimentally, mainly from the size of the braided sleeves.

The actual measured and theoretically calculated values for the length-width relationship of these frames are shown in Fig. 8(b). The results confirm that the calculated deformations of the cantilever beams are well representative of the actual deformations. The two types implemented in this research have approximately the same volume, and the plane muscles are more expansive. It can be said that the overall deformation can be designed with the size and number of deformed beams as parameters.

B. Tendon based on SAT

1) *Tendon Construction Method and Mechanical Characteristics:* As a tendon that can be used in a three-dimensional configuration, it should be thin and strong, with low friction on the surface and no interference during contact. It is also known that the stiffness can be changed by incorporating a nonlinear elastic element in the wire drive [22], which is important for expanding the range of robot motions. Stiffness Adjustable Tendon (SAT) [20] has already been proposed as a nonlinear elastic element with a tendon-like shape. By covering a silicon sponge with a braided tube, the braided sleeve is pulled and crushes the sponge's inside, resulting in nonlinear elasticity as a whole. This method is considered to

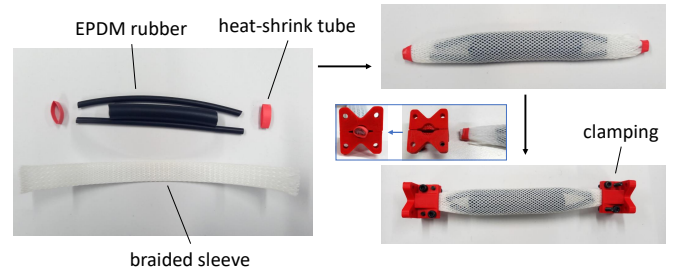


Fig. 9. Assembly of tendon based on SAT [20].

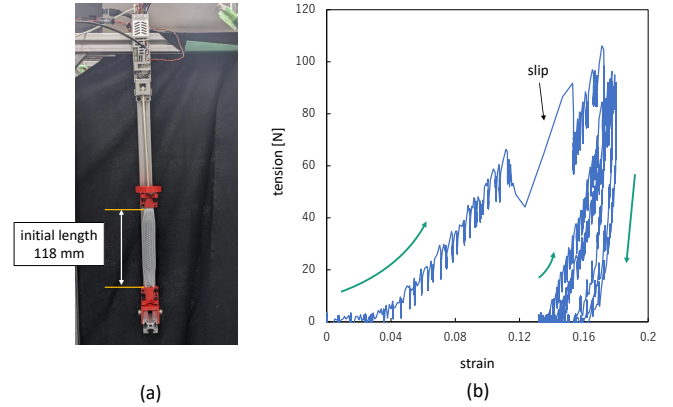


Fig. 10. (a) Tensile experiment of tendon based on SAT. (b) The elongation was large when the load was first applied. Slipping also occurred, but it did not come out of the fastener. After that, the strain remained within a narrow range.

be durable and can withstand contact at joints because the surface gap is smaller than that of conventional springs.

Therefore, in this study, we constructed an elastic element as a tendon based on the proposed SAT (Fig. 9). In order to make the element not only cylindrical in shape, several round rubbers are inserted inside and the ends of the sleeves are fastened in a plane shape.

Ethylene-propylene-diene (EPDM) rubber was used as the inner material. To keep the rubber from coming out, the end of the braided sleeve is covered with heat-shrinkable tubing and then heated to close it. Since the heated part becomes thicker, it should protrude outside the fastener during fastening to prevent it from falling out.

The relationship between load and strain of the tendon based on the SAT was examined when the vertical upward load was increased or decreased in steps by discretely changing the command current value to the motor (Fig. 10). The fastener occasionally slipped during the experiment but did not detach completely, as the endpoint was thicker than the fastener's hole. Although the elongation was large at the initial load increase due to the margin of the sleeve's shape, the strain was kept within a small range after that. The tendon, based on the SAT, has the required thinness and strength. The entire tendon is covered by the braided sleeve, which is thought to prevent interference even when the tendon contacts joints.

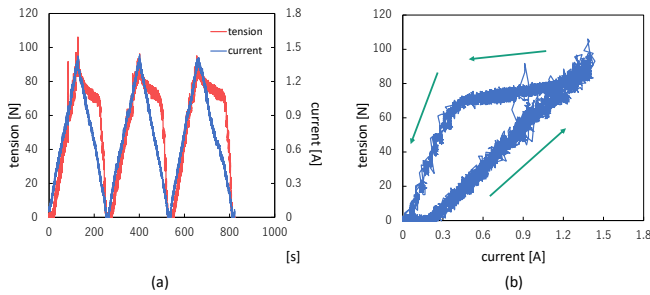


Fig. 11. (a) Time series of tension and current during tensile experiment. (b) Wire winding module has hysteresis in tension-current characteristics.

2) *Tension-Current Characteristics of Wire Winding Module*: In relation to the tensile experiments, we also report on the characteristics of the wire winding module by examining the relationship between the tension and the current. The time-series variation of tension and current is shown in Fig. 11(a), and the tension-current graph is shown in (b).

Ideally, the motor's exerted torque and the resulting wire tension are proportional to the motor current. When the current is increased, they are almost proportional to each other. However, when the current is decreased, the tension value does not decrease much, and a sharp decrease is observed from a certain value. Also, the tension value does not initially increase when the current increases.

This result is a characteristic of the wire winding module itself, and it can be said that a force resisting the direction of motion of the wire and the pulley is working. This is considered to be caused by the reduction gear in particular, and the effect is expected to be reduced by decreasing the reduction ratio.

Although not addressed in this research, the effect of hysteresis in the tension-current relationship must be considered for biological-like motion, including its impact on control. Hysteresis is expected to negatively affect fast movements, in which case the motor module needs to be improved.

III. EXPERIMENTS AND DISCUSSIONS

In this chapter, we evaluate whether the advantages of the muscle-tendon complex drive concept discussed and verified in the two-dimensional type of ww-MTC [1] are valid in three-dimensional motion, and whether the configuration proposed in this research is also effective in three-dimensional motion. Specifically, the following experiments will be conducted to verify the characteristics of the robot with 3D ww-MTC.

- We verify the robot's toughness (internal protection function) by applying disturbance with a hammer.
- We verify whether the muscles cooperate without interfering with each other by examining the change in stiffness when the tension is changed. We also examine the change in the appearance of the muscles in response to changes in tension.
- We examine the adaptability of this robot to contact with the environment by applying disturbance while moving the arm part.

A. 2-axis 3-muscle Robot Configuration

The robot used in the experiment is shown in Fig. 1(b). The joint modules used in Musashi [14] are used for the 2-axis joints. The module has a potentiometer inside to measure the angles. Since the actual value of the potentiometer is noisy, the joint angle graph in Section III-B is a calculated moving average.

The wire winding module is mounted far from the muscle. The ability to separate the drive from the actual force-activated part is an advantage of the wire drive. In this case, the space is open enough to connect the wires on the muscle exterior and the wires from the motor module, facilitating assembly and repair in case of wire breakage.

In mounting the ww-MTC, the tendons are adjusted to align around the joint without loosening when the roll and pitch are 0 degrees, and the muscle is around its natural length with no tension applied to the wires. Three ww-MTCs are attached to the two axes, and the tendon ends of two muscles (B, C) on the same side of the central link are attached at different positions to allow three-dimensional arm movement. In addition, a planar muscle is used for the medial muscle (B in Fig. 1(b)) in the area where the muscles overlap. This reduces the effect of the inner muscles pushing the outer muscles during deformation so that the muscles can cooperate effectively. This corresponds to the relationship between the brachialis and biceps muscles in the human body [23], for example.

B. Internal Protection

Muscle-tendon complexes are considered to have toughness in protecting themselves and the body when in contact with the environment. We conducted an experiment in which we hit each part of a 2-axis 3-muscle robot with a hammer (Fig. 12). There was no damage to ww-MTC, internal parts, or wires, and the toughness of the robot was confirmed.

In addition, a two-dimensional configuration using a muscle exterior with a single arch structure (Fig. 2) showed a rapid increase in tension when impact was applied [1], but this was not observed in the proposed configuration. Compared to the structure using only two PTFE plates, the muscle exterior composed of multiple PP sheets absorbs external forces without transferring them to the internal wires because of the structural margin that allows for distortion and deformation. This result indicates the high flexibility and safety of the proposed muscle exterior.

C. Stiffness and Appearance when Changing Tension

In order to verify the changes in stiffness and appearance, experiments were conducted to move the tip of the arm in various directions and then release it for the cases of low (Fig. 13) and high (Fig. 14) motor command current. In the high-tension case, moving the arm by hand force was difficult. Especially in the direction of roll, where the moment arm of the muscle is large, the arm hardly moves. In the two-dimensional ww-MTC [1], the muscles expanded too much and interfered with each other's movement, making it difficult to move even at low tension, and no change in

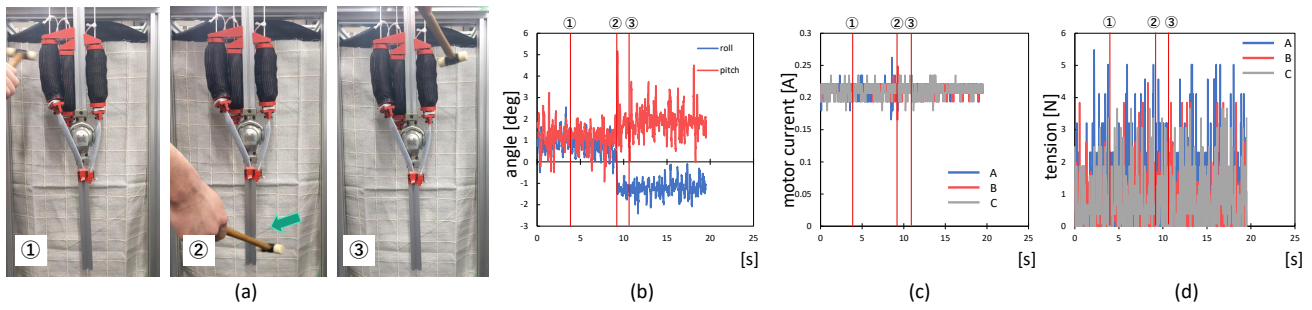


Fig. 12. The structure protects inner parts against hammering. (a) shows the scene of the hammer impact. (b)(c)(d) shows the time series of measured joint angle, motor current, and tension. The command current is constant.

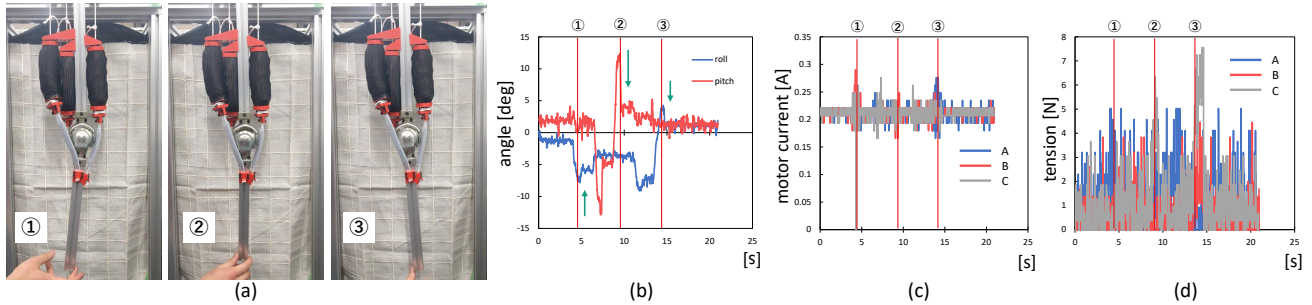


Fig. 13. 2-axis 3-muscle robot with low tension. (a) shows the scene before releasing the arm. (b)(c)(d) shows the time series of measured joint angle, motor current, and tension. The command current is constant. The arm part moves softly and then converges.

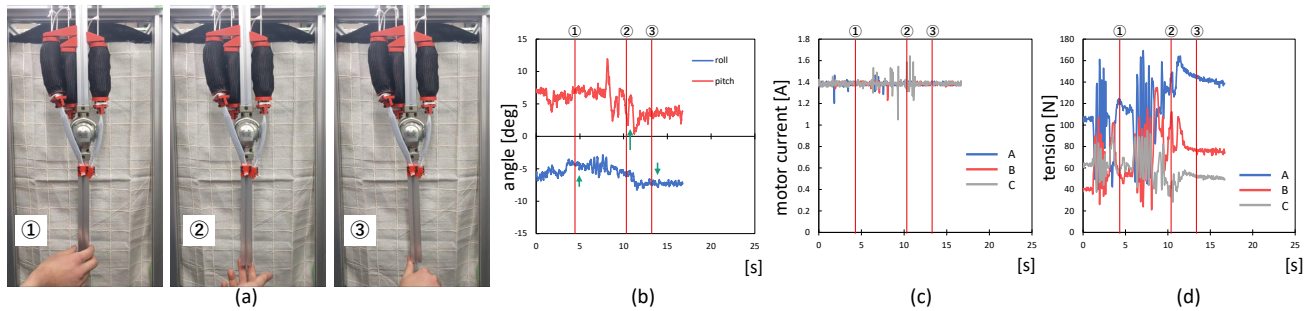


Fig. 14. 2-axis 3-muscle robot with high tension. (a) shows the scene before releasing the arm. (b)(c)(d) shows the time series of measured joint angle, motor current, and tension. The command current is constant. The arm part is almost motionless and converges immediately.

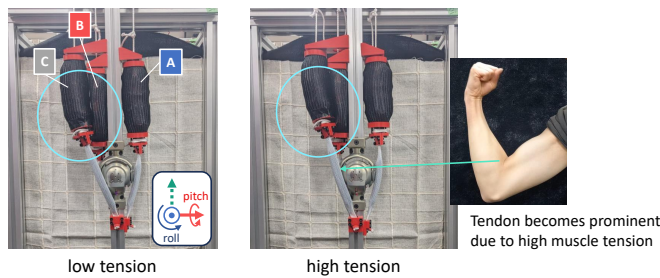


Fig. 15. When muscle tension is high, the muscle-tendon complex is pressed inward (the area indicated by the light blue circles). Also, the tendon becomes stretched and more visible.

stiffness was observed. On the other hand, in the present work, the change in the angle of the arm after the release indicates that the arm moves softly at low tension, while the

stiffness increases at high tension. These results show that the muscle expansion is gentle enough to allow the muscles to cooperate effectively.

In terms of appearance, the muscular appearance of the robot is useful for coexistence with humans by making the robot's state more visible. Comparing the still images in the two states, we can see that the lower end of the muscle is higher in the case of high tension (Fig. 15). In the higher tension case, the outer muscle (C) presses down on the inner muscle (B), and the tendon is more nearly parallel to the body axis. Although the expansion is not as visually apparent as in the two-dimensional ww-MTC constructed with PTFE (Fig. 2(b)), we can observe the difference through the elongation of the tendons. These differences may appear as wrinkles or shadows when the body structure, including the skin, is constructed, and further verification is needed.

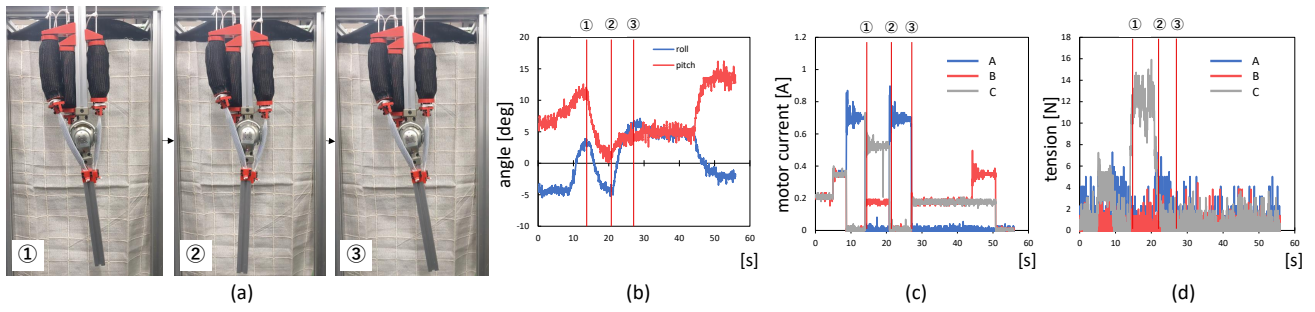


Fig. 16. Arm moving experiment without disturbances. (a) The robot arm can move in three-dimensional space. (b)(c)(d) shows the time series of measured joint angle, motor current, and tension. By changing the current command value, the tension on the wire changes, and the joint moves.

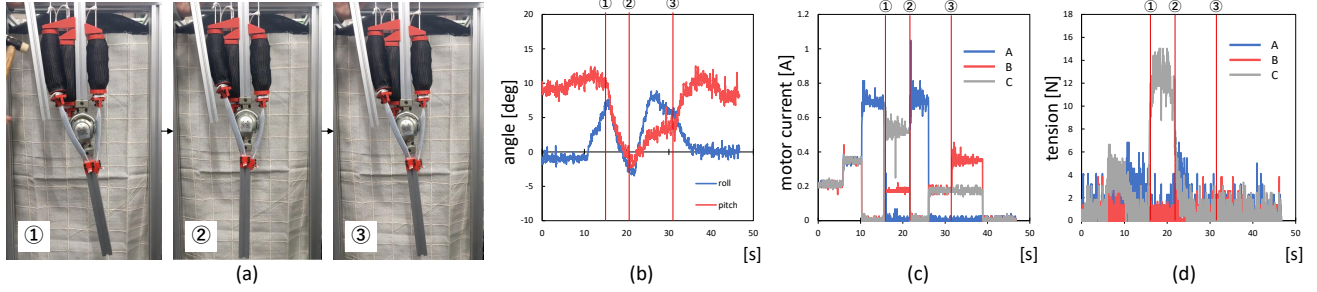


Fig. 17. (a) The robot maintains moving in spite of external disturbance. (b)(c)(d) shows the time series of measured joint angle, contraction length, and tension. By changing the current command value, the tension on the wire changes, and the joint moves. The trajectory of joint angles shows no sudden or unexpected changes during the disturbance experiments. The observed variations in the angle measurements remain consistent with the noise level seen in the undisturbed motion.

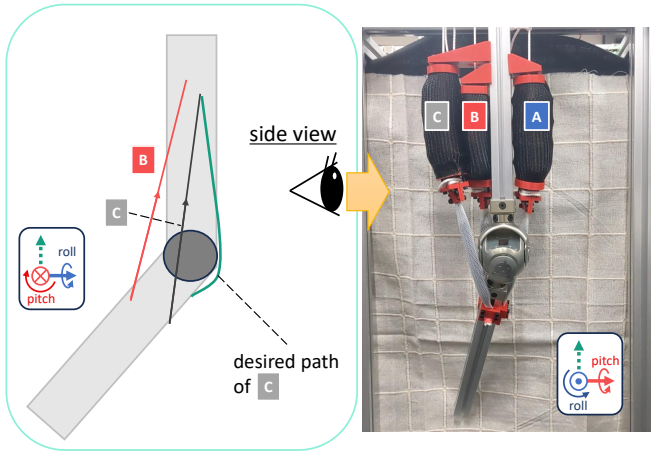


Fig. 18. The tendon path sometimes becomes dislocated from the joint.

D. Adaptability to Environmental Contact during Arm Movement

Motion experiments of a 2-axis 3-muscle robot were conducted, in which the arm part is swung.

The motion experiment without any disturbance is shown in the Fig. 16, and the muscles move while maintaining contact. On the other hand, a similar behavior was observed when the muscles were subjected to external disturbances such as pressing a square aluminum rod against them, shaking them with a surface pressed against them, or hitting them with a hammer (Fig. 17). The trajectory of joint angles does not show sudden or unexpected changes (Fig. 17(b)).

Although the external disturbance changed the position and shape of the muscles, they could continue to move while maintaining contact with each other.

As in the case of Fig. 12, no significant change in tension was observed, and both the muscles and tendons could continue to be used without any problems after the experiment. It is challenging to conduct disturbance experiments safely with standard wire drives because of the possibility of snagging and a sudden increase in tension. It is considered that the flexible deformable muscle exterior, which can be contacted on all surfaces, has enhanced the adaptability to environmental contact.

On the other hand, depending on the trajectory, the tendon's path may dislocate from the joint, as shown in Fig. 18, making it difficult to move in a certain direction. We used a joint module [14] that provides a wide range of motion similar to a spherical joint in a compact form. However, when using muscle-tendon complex drive in a three-dimensional configuration, it is necessary to design the structure of the joint part as well, taking the range of motion into consideration.

IV. CONCLUSION

This study developed a new muscle exterior to use the previously proposed wire-wound Muscle-Tendon Complex (ww-MTC) Drive in a three-dimensional body configuration. The deformation is controlled by the internal frame of the PP sheets and covered by a braided sleeve to realize a deformable muscle exterior that can be in contact with the entire surface. The consistency with theoretical calculations

is verified, and it is shown that the number and size of the sheets can adjust the muscle's deformation. In addition, a tendon as a thin and strong elastic element was constructed based on the previously proposed Stiffness Adjustable Tendon (SAT).

We applied these muscle exteriors and tendon elements to a 2-axis 3-muscle robot and verified their effectiveness in a three-dimensional workspace. The muscle exterior protected the robot's inner part and allowed it to adapt to environmental contact while continuing its movements flexibly. It is concluded that the muscle exterior and tendon elements in this study can be used in a three-dimensional configuration and enhance the adaptability of wire-driven robots to environmental contact.

In the future, we will realize various muscle shapes existing in the human body and establish a body configuration method using muscle-tendon complexes together with the design of joint parts. Furthermore, we aim to develop a humanoid robot suitable for environmental contact with its whole body and realize various motions by using the muscle-tendon complex drive.

REFERENCES

- [1] Y. Ribayashi, K. Miyama, A. Miki, K. Kawaharazuka, K. Okada, K. Kawasaki, and M. Inaba, "Development of a wire-wound muscle-tendon complex drive and its application to a two-dimensional robot configuration," in *Proceedings of the 2023 IEEE-RAS International Conference on Humanoid Robots*, 2023, pp. 758–764.
- [2] Fourier Intelligence, "GR-1," accessed: 2024-07-14. [Online]. Available: <https://fourierintelligence.com/gr1/>
- [3] PAL Robotics, "TALOS," accessed: 2024-07-14. [Online]. Available: <https://pal-robotics.com/robots/talos/>
- [4] APPTRONIK, "APOLLO," accessed: 2024-07-14. [Online]. Available: <https://apptronik.com/apollo>
- [5] IX, "NEO," accessed: 2024-07-14. [Online]. Available: <https://www.ix.tech/androids/neo>
- [6] N. Hiraoka, M. Murooka, H. Ito, I. Yanokura, K. Okada, and M. Inaba, "Whole-body control of humanoid robot in 3d multi-contact under contact wrench constraints including joint load reduction with self-collision and internal wrench distribution," in *2019 IEEE/RSJ International Conference on Intelligent Robots and Systems (IROS)*. IEEE, 2019, pp. 3860–3867.
- [7] F. Ruscelli, M. P. Polverini, A. Laurenzi, E. M. Hoffman, and N. G. Tsagarakis, "A multi-contact motion planning and control strategy for physical interaction tasks using a humanoid robot," in *2020 IEEE/RSJ International Conference on Intelligent Robots and Systems (IROS)*. IEEE, 2020, pp. 3869–3876.
- [8] P. Ferrari, L. Rossini, F. Ruscelli, A. Laurenzi, G. Oriolo, N. G. Tsagarakis, and E. M. Hoffman, "Multi-contact planning and control for humanoid robots: Design and validation of a complete framework," *Robotics and Autonomous Systems*, vol. 166, p. 104448, 2023.
- [9] J. Pratt, J. Carff, S. Drakunov, and A. Goswami, "Capture point: A step toward humanoid push recovery," in *2006 6th IEEE-RAS international conference on humanoid robots*. Ieee, 2006, pp. 200–207.
- [10] B. J. Stephens and C. G. Atkeson, "Push recovery by stepping for humanoid robots with force controlled joints," in *2010 10th IEEE-RAS International conference on humanoid robots*. IEEE, 2010, pp. 52–59.
- [11] V. B. Semwal, K. Mondal, and G. C. Nandi, "Robust and accurate feature selection for humanoid push recovery and classification: deep learning approach," *Neural Computing and Applications*, vol. 28, pp. 565–574, 2017.
- [12] S. Wittmeier, C. Alessandro, N. Bascarevic, K. Dalamagkidis, D. Devereux, A. Diamond, M. Jäntsch, K. Jovanovic, R. Knight, H. G. Marques, P. Milosavljevic, B. Mitra, B. Svetozarevic, V. Potkonjak, R. Pfeifer, A. Knoll, and O. Holland, "Toward Anthropomorphic Robotics: Development, Simulation, and Control of a Musculoskeletal Torso," *Artificial Life*, vol. 19, no. 1, pp. 171–193, 2013.
- [13] M. Jäntsch, S. Wittmeier, K. Dalamagkidis, A. Panos, F. Volkart, and A. Knoll, "Anthrob - A Printed Anthropomorphic Robot," in *Proceedings of the 2013 IEEE-RAS International Conference on Humanoid Robots*, 2013, pp. 342–347.
- [14] K. Kawaharazuka, S. Makino, K. Tsuzuki, M. Onitsuka, Y. Nagamatsu, K. Shinjo, T. Makabe, Y. Asano, K. Okada, K. Kawasaki, and M. Inaba, "Component Modularized Design of Musculoskeletal Humanoid Platform Musashi to Investigate Learning Control Systems," in *Proceedings of the 2019 IEEE/RSJ International Conference on Intelligent Robots and Systems*, 2019, pp. 7294–7301.
- [15] I. Mizuuchi, M. Kawamura, T. Asaoka, and S. Kumakura, "Design and development of a compressor-embedded pneumatic-driven musculoskeletal humanoid," in *2012 12th IEEE-RAS International Conference on Humanoid Robots (Humanoids 2012)*, 2012, pp. 811–816.
- [16] A. Hitzmann, H. Masuda, S. Ikemoto, and K. Hosoda, "Anthropomorphic musculoskeletal 10 degrees-of-freedom robot arm driven by pneumatic artificial muscles," *Advanced Robotics*, vol. 32, no. 15, pp. 865–878, 2018.
- [17] C.-P. Chou and B. Hannaford, "Measurement and modeling of mckibben pneumatic artificial muscles," *IEEE Transactions on Robotics and Automation*, vol. 12, no. 1, pp. 90–102, 1996.
- [18] B. Kalita, A. Leonessa, and S. K. Dwivedy, "A review on the development of pneumatic artificial muscle actuators: Force model and application," *Actuators*, vol. 11, no. 10, p. 288, 2022.
- [19] Y. Asano, T. Kozuki, S. Ookubo, K. Kawasaki, T. Shirai, K. Kimura, K. Okada, and M. Inaba, "A sensor-driver integrated muscle module with high-tension measurability and flexibility for tendon-driven robots," in *2015 IEEE/RSJ International Conference on Intelligent Robots and Systems (IROS)*, 2015, pp. 5960–5965.
- [20] T. Shirai and T. Tomioka, "Proposal of joint stiffness adjustment mechanism SAT -analysis and modeling of SAT-," in *Proceedings of JSME Conference on Robotics and Mechatronics (ROBOMECH '03)*, 2003, pp. 2P2–2F–F1, (in japanese).
- [21] R. Frisch-Fay, *Flexible Bars*. Butterworths, London., 1962.
- [22] K. Koganezawa, Y. Watanabe, and N. Shimizu, "Antagonistic muscle-like actuator and its application to multi-dof forearm prosthesis," *Advanced Robotics*, vol. 12, no. 7-8, pp. 771–789, 1997.
- [23] P. W. Tank and T. R. Gest, *Lippincott Williams & Wilkins Atlas of Anatomy*. Butterworths, London., 2009.